Surface Characterisation of α-, β-, γ-, and δ-UO_3 using *X*-Ray Photoelectron Spectroscopy *

Geoffrey C. Allen and Nigel R. Holmes
Central Electricity Generating Board, Berkeley Nuclear Laboratories, Berkeley, Gloucestershire GL13 9PB

X-Ray photoelectron spectroscopy, i.r. spectroscopy, and *X*-ray diffraction have been used to characterise the higher oxides α-, β-, γ-, and δ-UO_3. While the i.r. and *X*-ray diffraction results may be used to characterise each oxide, the *X*-ray photoelectron spectra for the four phases are very similar. During reduction of the oxide surface in the spectrometer, changes in the spectra were observed which were shown to be associated with particular oxidation states of the metal rather than different uranium atom co-ordination sites within the oxide. A close structural relationship is demonstrated between these oxides and the product at the surface of air-oxidised UO_2 fuel.

The chemistry of nuclear fuel is dominated by the ability of UO_2 to accommodate oxygen up to the stoicheiometric composition UO_3. Between these two extremes some twenty or so phases have been reported. In recent years our understanding of the complex structure of the hyperstoicheiometric phases of UO_2 has been considerably improved by the use of spectroscopic techniques.[1] Previous reports have concentrated on the lower members of the series between UO_2 and U_2O_5, but above the midpoint the region stretching to UO_3 is dominated by the stable orthorhombic structure of U_3O_8.

In 1961 Hoekstra *et al.*[2] presented evidence to show that the oxidised surface layer which forms on UO_2 at 25 °C is amorphous UO_3. Thus to complete our investigation of the surface properties of nuclear fuel and its oxidation products here we concentrate on a characterisation of the oxides above U_3O_8, namely the uranium trioxide species α-, β-, γ-, and δ-UO_3, by *X*-ray photoelectron spectroscopy (x.p.s.), i.r. spectroscopy, and *X*-ray diffraction.

Experimental

X-Ray Photoelectron Spectra.—The instrument used in this work was an AEI ES200B photoelectron spectrometer operated in the fixed analyser transmission (f.a.t.) mode with a pass energy of 65 eV. The base pressure of the spectrometer was of the order of 10^{-11} Torr, and most spectra were obtained at 10^{-9} Torr with unmonochromatised Al-K_α radiation (1 486.6 eV). The anode was routinely operated at 240 W (12 kV, 20 mA) with the source and collector slits set to 0.060 and 0.070 in, giving a peak full width at half maximum height (f.w.h.m.) of 1.15 eV for the gold $4f_{\frac{7}{2}}$ peak.

Calibration was achieved using the copper $2p_{\frac{3}{2}}$ peak at 932.67 eV, the gold $4f_{\frac{7}{2}}$ peak at 84.00 eV, and the nickel Fermi level.[3] These metal foils were prepared by etching with an Ion-tech FABS gun at 6 kV and 20 μA using BOC Research Grade argon. Spectra for the U 4*f*, O 1*s*, C 1*s*, and valence regions were recorded with a DEC PDP 11-23 minicomputer. Results were stored using Kratos DS800 software.

Calibration of Insulators.—The accurate calibration of photoelectron spectra taken from an insulating sample is complicated by charging at the surface which shifts all the binding energies to higher values. Such charging may produce a shift of the order of 3—10 eV, compared with a typical chemical shift of 1—3 eV. A reference binding energy for an insulating surface may be obtained by gold evaporation.[4] However, the binding energy recorded from the gold layer may vary by up to 1.3 eV depending on the size of the deposited gold clusters,[5,6] the amount of gold deposited,[7] and the nature of the substrate.[8] For this reason, calibration in the present work was achieved by referring to the C 1*s* binding energy of adventitious carbon at 285.0 ± 0.3 eV.[9] This is carbon contamination which builds up on the surface from the residual gases in the ultra high vacuum (u.h.v.) chamber. The C 1*s* binding energy of adventitious carbon on a UO_2 surface has been measured at 285.0 eV.[10] Although UO_2 is a semiconductor, we have taken the binding energies of adventitious carbon on UO_2 and UO_3 to be similar and use the above value as our reference in this work.

Sample Preparation.—Samples of α-, β-, γ-, and δ-UO_3 were prepared, characterised, and kindly supplied by Dr. P. G. Dickens of the University of Oxford. Initially the γ-UO_3 sample used was from Koch-Light Laboratories, 99.5% purity. However, the x.p.s. results from this gave much higher U 4*f* and O 1*s* binding energies than did the other three polymorphs studied. The γ-UO_3 sample was then characterised by i.r. spectroscopy and *X*-ray diffraction, which showed that it had become contaminated with water. The i.r. spectrum showed two intense peaks at 960 and 940 cm^{-1} characteristic of uranyl-type bonding which is absent in γ-UO_3. The *X*-ray diffraction pattern was similar to that given by Dawson *et al.*[11] for a sample of $UO_3 \cdot 0.8\ H_2O$ but also showed some very weak peaks from γ-UO_3.

To obtain a sample of γ-UO_3 the contaminated γ-UO_3 sample was heated at 300 °C for 24 h in a stream of dry air. The weight of the sample was recorded before and after heating. This showed a weight loss of 23.63 mg from an initial sample weight of 487.84 mg. Assuming that the product is UO_3 and that the contamination was due to water, then the starting material was formulated as $UO_3 \cdot 0.81\ H_2O$.

The product was characterised by i.r. spectroscopy and *X*-ray diffraction. The i.r. spectrum showed the absence of peaks at 960 and 940 cm^{-1} (see Figure 1) and the *X*-ray diffraction pattern could be indexed on the pattern given by Engmann and de Wolff[12] for a sample of γ-UO_3 (see Figure 2). There was also a change in colour from the pale yellow starting material to the orange product. No further change in the colour of the product was observed after 4 weeks in a stoppered sample bottle.

Several methods of mounting the UO_3 powder were tried, including spreading it over copper-backed adhesive tape (3M company), double-sided Lomacoll tape, and pressing it into indium foil. Using these methods the spectra showed uneven charging across the sample (giving wide U 4*f* peaks) and peak contributions from the backing material. To overcome these

* *Non-S.I. units employed:* eV ≈ 1.60 × 10^{-19} J, Torr ≈ 133 Pa, in = 2.54 × 10^{-2} m.

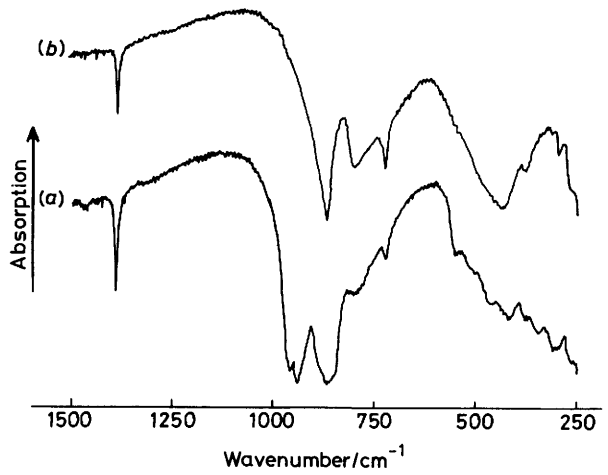

Figure 1. I.r. spectra (1 500—250 cm^{-1}) of (*a*) the original γ-UO_3 sample and (*b*) the heated γ-UO_3 sample

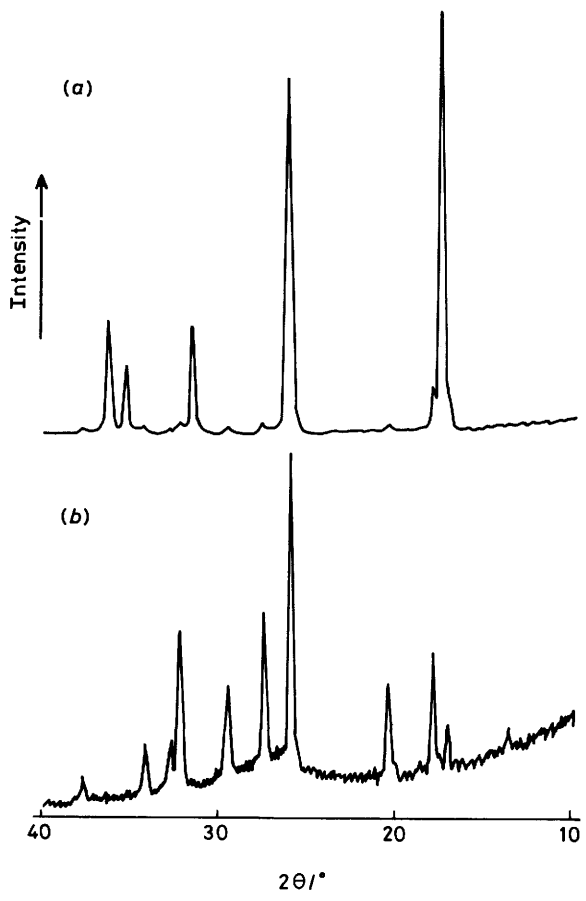

Figure 2. *X*-Ray diffraction spectra for the samples in Figure 1

problems the UO_3 powder was pressed into a pellet which completely covered the probe tip.

Pellets of UO_3 were produced by compacting about 2 g of powder in a 13-mm die press at a pressure of 5 000 kg (3.4 MPa). There was a noticeable change in colour in pressing the δ-UO_3 pellet; δ-UO_3 has the lowest theoretical density of the UO_3 phases and might be expected to be the least stable under pressure. This was checked by taking the powder *X*-ray diffraction spectra before and after pelleting at 10 000 kg (6.7 MPa). The results showed the δ-UO_3 phase to be unchanged. The pellets were 1.5—2 mm thick and 13 mm in diameter. They were trimmed to a width of 10 mm to allow insertion through the poly(tetrafluoroethylene) (ptfe) seals on the insertion lock. The pellet was fixed to a 6 mm wide copper probe tip using Lomacoll double tape so that the probe tip was covered by the pellet. Before insertion into the spectrometer the pellet was scraped with a sharp blade to expose fresh oxide.

Results and Discussion

Structures of the UO_3 *Phases.*—In UO_3 phases the uranium atom may be co-ordinated to six, seven, or eight surrounding oxygen atoms, leading to at least six polymorphs.[13,14]

The α-UO_3 phase can be regarded as a uranium-deficient form of α-U_3O_8. Introduction of uranium vacancies into the latter[15] re-establishes an O:U ratio of 3:1. Approximately one quarter of the oxygen atoms within the O–U–O–U–O chains are co-ordinated to one rather than two uranium atoms,[16] shortening the U–O distance from 2.08 to 1.64 Å and giving the bond some 'uranyl' or double-bond character. This correlates with an observed ν_3 asymmetric stretching frequency at 935 cm^{-1}.[17,18]

The structure of β-UO_3 contains three distinct types of uranium atom[19] in a unit cell containing 10 uranium atoms: U(1) has a distorted octahedral co-ordination, U(2) and U(3) each have six oxygen neighbours, and U(4) and U(5) are seven-co-ordinate. Two of the oxygen atoms co-ordinated to U(2) and U(3) are considered to form an uranyl group, which has the unusual O–U–O bond angle of 150°.[20] Two absorptions are observed in the i.r. spectrum at 936 and 965 cm^{-1} which can be assigned to a uranyl group.[17]

The structure of γ-UO_3 is pseudo-tetragonal with two distinct types of uranium atom:[21] U(1) has a distorted octahedral co-ordination, while U(2) has dodecahedral co-ordination. At room temperature the shortest U–O distance is 1.796 Å which suggests the absence of pure uranyl bonds. This is in accord with the i.r. spectrum of γ-UO_3 from which the ν_3 asymmetric stretch at 910—960 cm^{-1} is absent.[22]

The δ-UO_3 phase adopts the ReO_3 structure[23] in which UO_6 octahedra are linked together to form a framework of stoicheiometry UO_3. All of the uranium atoms are in a regular octahedral co-ordination, and there is no evidence for the presence of uranyl groups.

The co-ordination around the uranium atoms in the above phases is summarised in Table 1. The i.r. spectra of the samples used are given in Figure 3.

Core-level Binding Energies in UO_3.—The results of eight previous x.p.s. studies of UO_3 are collected and summarised in Table 2. There is a spread of binding energy values for the U 4$f_{\frac{7}{2}}$ peak from 380.7 to 382.4 eV. The mean value from seven studies is 381.6 eV. The O 1*s* binding energy is quoted only in three cases, with values of 529.8, 530.0, and 531.4 eV. The spread in the results is probably due to the alternative methods used to obtain a reference binding energy, the different methods of mounting the specimen, and the varying conditions in other spectrometers.

The binding energies and peak widths for the O 1*s* and U 4*f* core electrons obtained in this work are presented in Table 3. Both the O 1*s* and U 4*f* binding energies for the α-, β-, γ-, and δ-UO_3 phases are very similar (see Figures 4 and 5), with the U 4$f_{\frac{7}{2}}$ peak binding energies ranging from 381.95 to 382.1 eV and the O 1*s* peak from 531.0 to 531.05 eV. These similarities

Table 1. Structural details of α-, β-, γ-, and δ-UO_3

Phase	α	β	γ	δ
Colour	Tan	Orange-red	Yellow, orange	Brick-red
Structure type	Defect orthorhombic	Monoclinic	Orthorhombic	Cubic
Uranium co-ordination sites	7, 8	6, 7	6, 8	6
Site geometries	7: Pentagonal bipyramidal 8: Hexagonal bipyramidal	Not known precisely	6: Distorted octahedral 8: Distorted dodecahedral	6: Regular octahedral
Presence of 'uranyl' group	Yes	Yes	No	No
Heat of formation,[2] ΔH_f(298 K)/kJ mol^{-1}	1 235	1 235	1 240	1 235

Table 2. Reported binding energies for UO_3

Author ref.	Phase	U 4$f_{\frac{7}{2}}$ Binding energy/eV	Satellites	U 4$f_{\frac{7}{2}}$ Binding energy/eV	F.w.h.m./ eV	O 1s Binding energy/eV	F.w.h.m./ eV	Ref. Binding energy/eV		Comments
a	A[b]	392.7 ± 0.1		381.9	3.0			Gold	84.0	
c	γ	392.6 ± 0.3		381.9	3.2	528.9	2.5	Deposited gold	84.0	
26	γ	391.4 ± 0.1		380.7	1.4			Deposited gold	83.8	*d*
27	γ	393.3 + 0.2[e]	3.9, 9.5	382.4	1.5	531.4	—	Pump oil	285.0	*d*
f	β	392.5 ± 0.1		381.5	2.4			Pump oil	285.0	*g*
h	α	392.2 ± 0.2		381.3	2.4			Pump oil	285.0	
24	γ		3.7, 10.6							*i*
j	—	392.4 ± 0.6		381.6	—	530.0	—	Gold	83.8	*k*

[a] D. Chadwick and J. Graham, *Nature (London)*, 1972, **237**, 127. [b] A = Amorphous. [c] G. C. Allen, J. A. Crofts, M. T. Curtis, P. M. Tucker, D. Chadwick, and P. J. Hampson, *J. Chem. Soc., Dalton Trans.*, 1974, 1296. [d] Uses monochromated *X*-rays with an electron flood gun for charge neutralisation. [e] Value estimated from the data of ref. 27. [f] R. Delobel, H. Baussart, J. M. Leroy, J. Grimbelot, and L. Gengembre, *J. Chem. Soc., Faraday Trans. 1*, 1983, 879. [g] Sample prepared by heating commercial UO_3 to 400 °C in a dynamic vacuum. [h] J. L. G. Fierro, E. Salazar, and J. A. Legarreta, *Surf. Interface Anal.*, 1985, **7**, 97. [i] Sample contaminated with nitrogen from starting material. [j] L. Feve, R. Fontaine, and M. J. Guittet, *C.R. Acad. Sci.*, 1982, **295**, 979. [k] Mentions sample preparation by argon-ion bombardment.

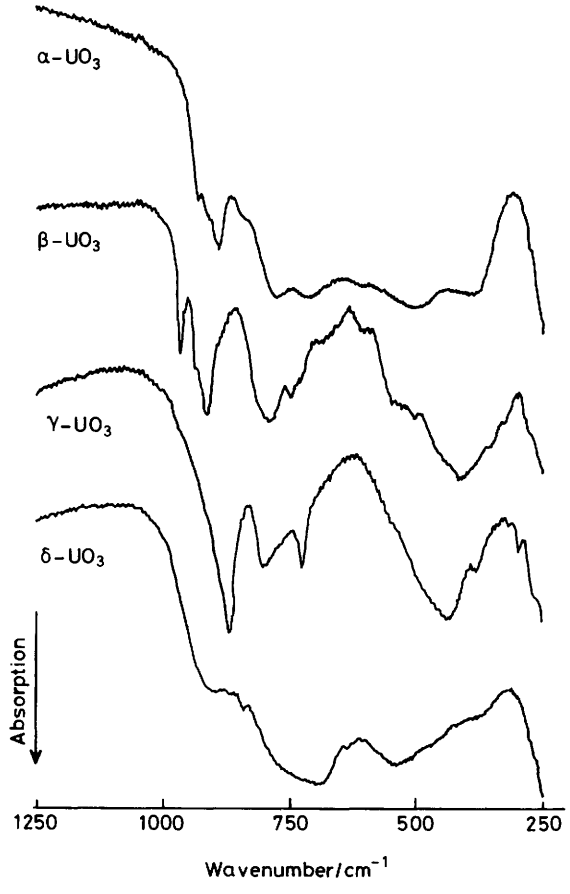

Figure 3. I.r. spectra (1 250—250 cm^{-1}) for the phases of UO_3

between the U 4*f* and O 1*s* binding energies were not expected, given the wide range of structure types and uranium co-ordination sites. However, the heats of formation of the four phases are almost identical (Table 1), and consideration of the Born–Haber cycle for the formation of UO_3 shows that the crystal-lattice energies for these phases will also have very similar values.

The changes in the binding energy of a core level are due to the free-ion shift and the crystal-field shift. For all of the UO_3 samples the free-ion shift is the same, due to U^{6+} and O^{2-} ions. The crystal-field shift is the effect of the surrounding ions on the binding energies, and it is associated with the partial Madelung potential of a given site in the lattice. As the crystal-lattice energies are so similar, the Madelung constants for the different phases must also have the same values. In view of this, the crystal-field shifts in α-, β-, γ-, and δ-UO_3 would also be expected to be closely similar.

The ionic model would account for the lack of differences between the photoelectron spectra of the different UO_3 phases studied here, but it does not take into account any covalent bonding that might occur in these oxides.

U 4*f* *Core-level Satellites.*—All four phases show U 4*f* satellites in similar positions with separations of *ca.* 4 and *ca.* 10 eV from the main peak, and the use of these features as an indicator of the presence of U^{VI} has been discussed by other workers.[24]

It is interesting that the satellite positions of UO_3 do not appear to be sensitive to changes in co-ordination of the uranium atom. The spectra of the α- and β-UO_3 phases in which 'uranyl' groups are thought to be present are very similar to the spectrum recorded from the γ- and δ-UO_3 phases in which this grouping is thought to be absent. This is a factor which tends to counter the view that the low-energy (*ca.* 3 eV) satellites may be attributed to charge transfer within a UO_2^{2+} or 'uranyl' group.

Table 3. Binding energies (eV) of U $4f_{\frac{5}{2}}$, $4f_{\frac{7}{2}}$, O 1*s* core levels in UO_3

Sample	U $4f_{\frac{5}{2}}$	U $4f_{\frac{7}{2}}$	F.w.h.m.	Satellites from U $4f_{\frac{5}{2}}$ peak centre	O 1*s*	F.w.h.m.
α-UO_3	392.95	382.1	1.95	10.0, 4.0	531.05	2.4
β-UO_3	392.85	382.0	1.95	9.6, 3.7	531.0	2.5
δ-UO_3	392.8	381.95	1.9	9.7, 4.0	531.0	2.4
γ-UO_3	392.95	382.0	1.9	9.8, 3.6	531.05	2.3

The accuracy of the values for the U 4*f* and O 1*s* peaks is ±0.25 eV based on C 1*s* (adventitious carbon, 285.0 ± 0.15 eV) and a measurement precision of ±0.10 eV. The satellites we measured relative to the centre of the U $4f_{\frac{5}{2}}$ peak measurement precision of ±0.10 eV and a satellite measurement precision of ±0.2 eV. The f.w.h.m. for the uranium core-level peaks is measured from the U $4f_{\frac{7}{2}}$ peak with no background subtraction.

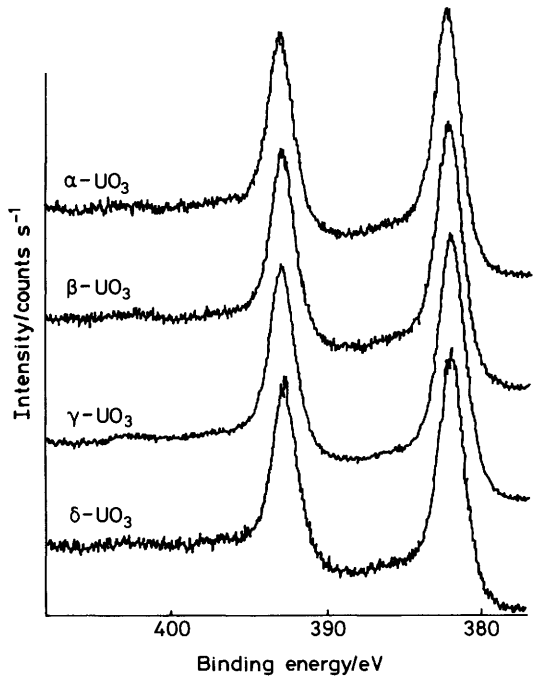

Figure 4. *X*-Ray photoelectron spectra of the uranium 4*f* core levels

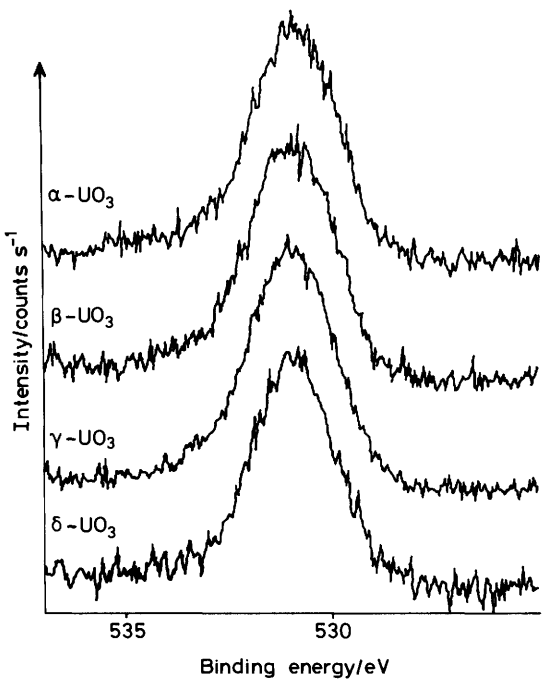

Figure 5. *X*-Ray photoelectron spectra of the oxygen 1*s* core levels

McGlynn and Smith[25] have stressed the significance of π bonding in the UO_2^{2+} grouping and thus assigned these low-energy transitions to an excitation of an electron from the highest-filled π orbital to a non-bonding orbital on uranium. However, such features persist at *ca.* 4 eV in the spectroscopic measurements for all of the compounds studied despite the fact that 'uranyl' bonding is absent in γ- and δ-UO_3. This suggests that the satellite positions may be dependent on the oxidation state of the uranium atom rather than on the nature of its co-ordination.

Both the U 4*f* satellites are attributed to charge transfer from the uranium–oxygen bonding band at *ca.* 5 eV below the Fermi level. A transition to the empty U 5*f* orbital at *ca.* 1.6 eV below the Fermi level produces the satellite at 4 eV. Similarly a transition to the U 6*d* conduction band at *ca.* 5 eV above the Fermi level is attributed to the satellite at 10 eV.

A spectrum of the α-UO_3 U 4*f* region is shown in Figure 7. This shows two satellites associated with the U 4*f* peaks at 4 and 10 eV. These satellite positions are in general agreement with those determined by both Verbist *et al.*[26] and Teterin *et al.*[27] (see Table 2). U 4*f* Satellites at 9.4—10.3 eV have also been observed in the spectra of the alkali-metal uranates.[28]

Reduction of UO_3 *Samples in Vacuum.*—The intensity of the U 4*f* satellites is only about 8% of the parent peak. Thus, to obtain an acceptable signal-to-noise ratio spectra were collected over long periods of time. A complete spectrum of the U 4*f* region could be acquired in 30 min, but detailed spectra of the satellite region required up to 2 h. During such measurements, a gradual decrease in the binding energy of both the U 4*f* and O 1*s* peaks was noticed, together with a broadening of the U 4*f* levels. There was also a change in the positions and intensities of the U 4*f* peak satellites, and the gradual appearance of the U 5*f* peak was also observed. The results obtained from an α-UO_3 pellet over a period of 16 h are collected in Table 4, and the series of spectra for the U $4f_{\frac{7}{2}}$ peak, the U 4*f* peak satellites, and the U 5*f* peak are shown in Figures 6, 7, and 8. All of these changes are due to reduction of the UO_3 pellet surface during *X*-ray bombardment under u.h.v. conditions.

The oxygen:uranium ratio may be determined by a comparison of the O 1*s* and U $4f_{\frac{7}{2}}$ peak areas. However this assumes that the O 1*s* peak is wholly due to the oxide and excludes the possibility of contributions from adsorbed water or CO_2. Under such circumstances a better method of estimating these ratios is through comparison of the 0—10 eV valence region of the

Table 4. Changes in the U 4*f*, U 5*f*, and O 1*s* peaks of α-UO_3 on exposure to *X*-rays and vacuum

Exposure time/h	1	3	7	15
Binding energy/eV				
U $4f_{\frac{5}{2}}$	393.0	392.8	392.55	392.5
U $4f_{\frac{7}{2}}$	382.1	382.0	381.75	381.65
F.w.h.m./eV of U $4f_{\frac{7}{2}}$	1.95	2.0	2.2	2.3
Satellites, distance from U $4f_{\frac{5}{2}}$ peak centre	10.0, 4.0	decreasing intensity ⟶	7.4	
U 5*f* peak height relative to U–O bonding band as a percentage	1.3	20.0	36.3	47.5
Binding energy/eV of O 1*s*	531.1	531.0	530.85	530.65
F.w.h.m./eV of O 1*s*	2.5	2.5	2.55	2.4

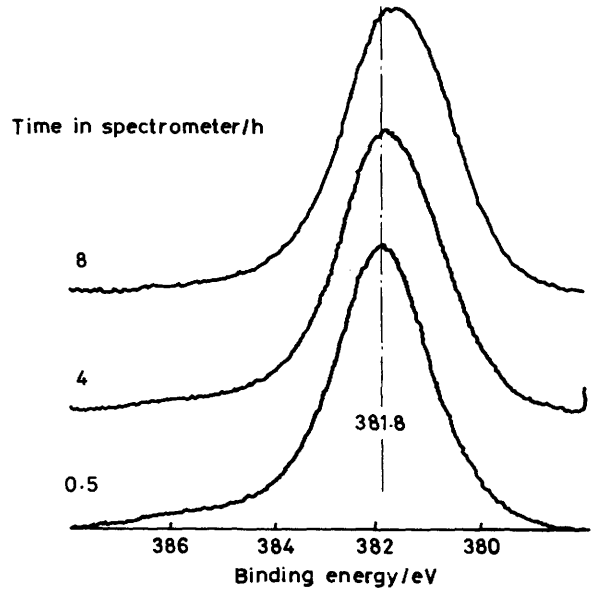

Figure 6. Changes in the U $4f_{\frac{7}{2}}$ peak shape of α-UO_3 during reduction

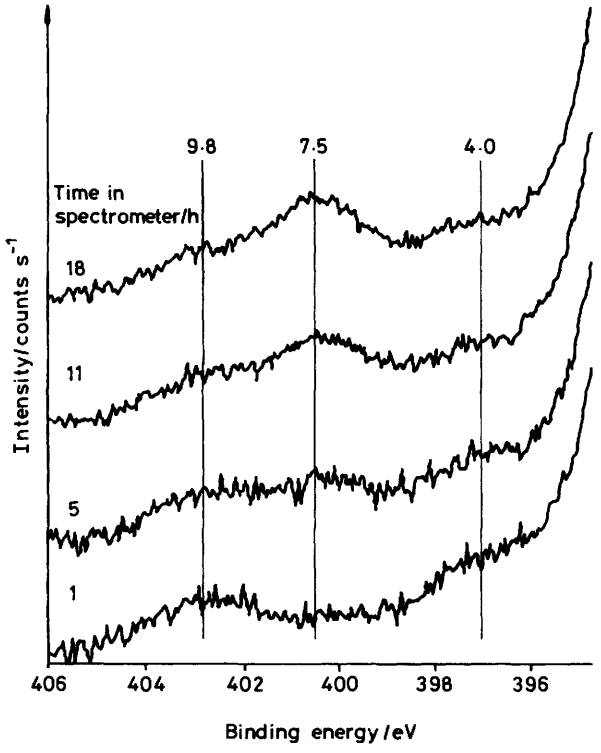

Figure 7. Changes in the intensities of the uranium 4*f* peak satellites (separations from the U $4f_{\frac{7}{2}}$ peak centre given in eV) observed during reduction of an α-UO_3 pellet

photoelectron spectrum recorded from the reduced oxide, with that from well characterised samples of UO_3, U_3O_8, U_3O_7, and UO_2. This shows the gradual change in the U 5*f* peak intensity on going from the $5f^0$ electronic configuration in UO_3 to the $5f^2$ configuration in UO_2.

A comparison of the valence-band spectrum of the reduced UO_3 with known oxides shows that after 14 h in the spectrometer the composition of the surface is approximately U_3O_8.

The reduction of a surface layer of the UO_3 pellet was demonstrated by scraping the pellet with a sharp blade. By this means a new layer of oxide was exposed which had a spectrum almost identical to that recorded when the pellet was first put into the spectrometer. This was the case for all the phases studied here. Reduction of the pellet surface lowered the U 4*f* and O 1*s* binding energies by about 0.5 eV for all the UO_3 phases. At the same time a gradual increase in the intensity of the 5*f* peak was observed at *ca.* 1.6 eV above the Fermi level, as would be expected if the outer electronic configuration of the uranium atom changed from $5f^0$ (U^{VI}) to either $5f^1$ (U^V) or $5f^2$ (U^{IV}). Similarly the broadening of the U 4*f* core levels can be explained by a gradual increase in the concentration of U^V or U^{IV} in the oxide lattice. In earlier x.p.s. studies, U_3O_8 was considered to be best described as $U^{IV}U^{VI}{}_2O_8$, and this compound gave U 4*f* levels which could readily be resolved into two component U^{IV} and U^{VI} peaks. On reduction in vacuum the U 4*f* peak profiles altered and an increase in the lower-binding-energy component was noted, corresponding to an increase in the amount of U^{IV} present in the reduced oxide.[10]

An analysis of the U 4*f* peak satellites in U_3O_8 is complicated by the composite nature of the core levels. However there appears to be one satellite at 8.2 eV from the component U^{IV} $4f_{\frac{7}{2}}$ and two satellites at 3.8 and 9.4 eV due to the component U^{VI} $4f_{\frac{7}{2}}$. Upon reduction of the U_3O_8 pellet the satellites at 3.8 and 9.4 eV are reduced in intensity, while the intensity of the satellite at 8.2 eV is increased (Figure 9).

Similar behaviour occurs when the UO_3 pellets are reduced. In the case of α-UO_3 no satellite was observed at 7.5 eV initially, but this feature appeared following exposure to *X*-rays. A corresponding reduction in the intensity of the two satellites associated with U^{VI} at 4 and 9.8 eV also occurred (see Figure 7).

Reduction of UO_3 could result in either a sub-stoicheiometric

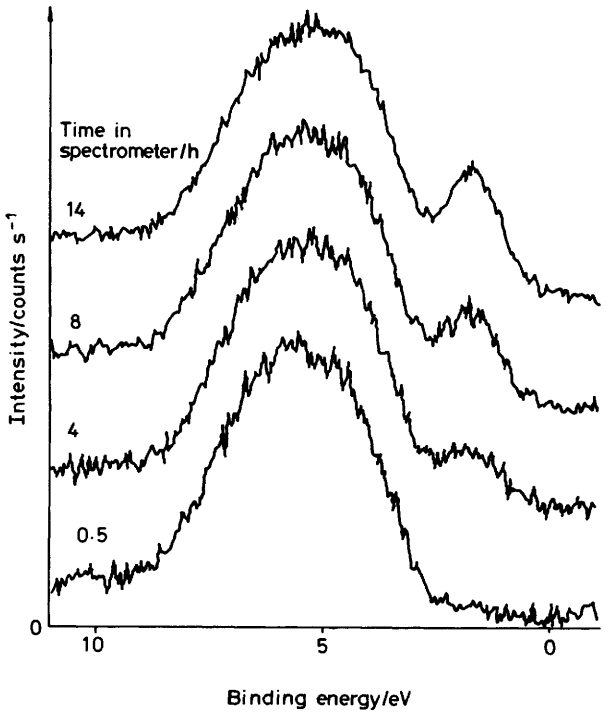

Figure 8. Changes in the valance-band and uranium 5*f* level observed during reduction of an α-UO_3 pellet

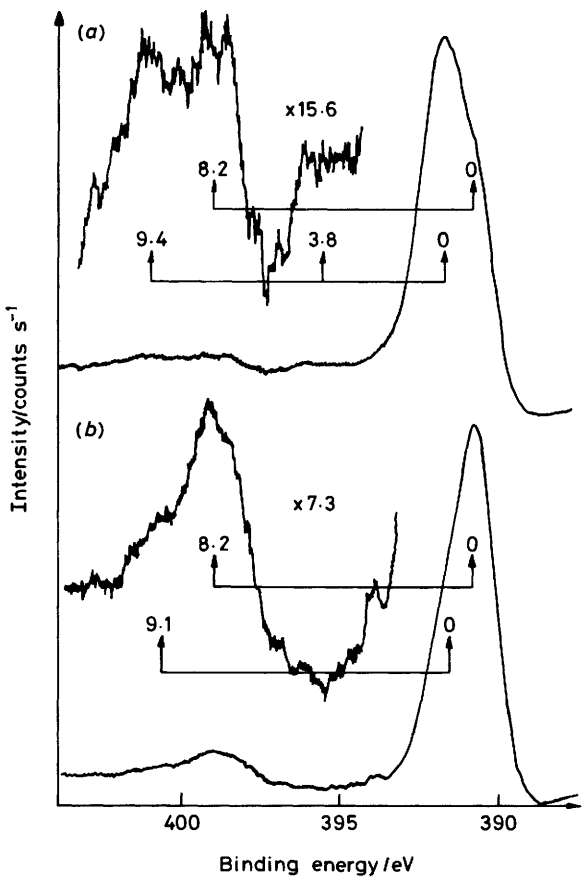

Figure 9. *X*-Ray photoelectron spectra of the U 4*f* region for U_3O_8: (*a*) fresh sample after insertion into the spectrometer; (*b*) same sample after reduction in vacuum. Separations between the U $4f_{\frac{7}{2}}$ peak centre and the satellites are given in eV

UO_{3-y} phase, or a mixture of oxides such as UO_3 and U_3O_8. The structural chemistry of the binary uranium oxides can be rationalised in terms of two distinct lattice types, the fluorite structure of UO_2 and the orthorhombic structure of U_3O_8.[29] Above U_3O_8, superstructures of the basic O–U–O–U layered structure extend the series to α-UO_3, and Hyde[30] has suggested that these two structures are, in fact, related by a crystallographic shear process. Starting with α-UO_3 he considered that, during reduction, a combination of crystallographic shear and ordered point defects would produce regions of U_3O_8 interwoven within the α-UO_3 parent lattice.

Conclusions

(1) Uranium trioxide exhibits a unique *X*-ray photoelectron spectrum which is sensitive to changes in stoicheiometry.

(2) It is not possible to differentiate between α-, β-, γ-, or δ-UO_3 using x.p.s.

(3) Reduction of the UO_3 surface is caused by exposure to *X*-rays under the conditions in the spectrometer.

(4) Changes in stoicheiometry can be followed by monitoring the U 4*f*, O 1*s*, and valence-band regions. There are also changes in the satellites associated with the U 4*f* peaks on reduction of an α-UO_3 sample.

(5) The satellites associated with the U 4*f* peaks have been analysed by assigning particular satellites to different oxidation states of uranium. In this study, satellites at 4 and 10 eV are due to U^{6+}, and a satellite at 7.5—8 eV appears to be associated with a reduced metal ion, probably U^{4+}.

(6) The positions of the satellites associated with the U 4*f* peaks in α-, β-, γ-, and δ-UO_3 are not affected by the co-ordination site of the uranium atom, or by the presence of 'uranyl' bonding in the oxide lattice.

Acknowledgements

This work was carried out at the Berkeley Nuclear Laboratories of the Technology Planning and Research Division and the paper is published with permission of the Central Electricity Generating Board.

References

1 G. C. Allen and P. A. Tempest, *Proc. R. Soc. London, Ser. A*, 1986, **406**, 325.
2 H. R. Hoekstra, A. Santoro, and S. Siegel, *J. Inorg. Nucl. Chem.*, 1961, **18**, 166.
3 M. T. Anthony and M. P. Seah, *Surf. Interface Anal.*, 1984, **6**, 95.
4 D. J. Hnatowich, J. Hudis, M. L. Perlman, and R. C. Ragaini, *J. Appl. Phys.*, 1971, **42**, 4883.
5 A. Fritsch and P. Légaré, *Surf. Sci.*, 1985, **162**, 742.
6 M. G. Mason, *Phys. Rev. B.*, 1983, **27**, 748.
7 Y. Uwamino, T. Ishizuka, and H. Yamatera, *J. Electron Spectrosc.*, 1981, **23**, 55.
8 S. Kohiki and K. Oki, *J. Electron Spectrosc.*, 1985, **36**, 105.
9 P. Swift, *Surf. Interface Anal.*, 1982, **4**, 47.
10 G. C. Allen, P. M. Tucker, and J. W. Tyler, *Vacuum*, 1982, **32**, 481.
11 J. K. Dawson, E. Wait, K. Alcock, and D. R. Chilton, *J. Chem. Soc.*, 1956, 3531.
12 R. Engmann and P. M. de Wolff, *Acta Crystallogr.*, 1963, **16**, 993.
13 H. R. Hoekstra and S. Siegel, *J. Inorg. Nucl. Chem.*, 1961, **18**, 154.
14 W. R. Cornman, AEC Report DP-749, E. I. Dupont de Nemours, Savannah River Laboratory, Aiken, South Carolina, 1962.

15 B. O. Loopstra, *Acta Crystallogr.*, 1964, **17**, 651.
16 C. Greaves and B. E. F. Fender, *Acta Crystallogr., Sect. B*, 1972, **28**, 3609.
17 R. Tsuboi, M. Tereda, and T. Shimanouchi, *J. Chem. Phys.*, 1962, **36**, 1301.
18 J. I. Bullock, *J. Chem. Soc. A*, 1969, 781.
19 P. C. Debets, *J. Inorg. Nucl. Chem.*, 1963, **26**, 1468.
20 S. V. Hawke, Part II Thesis, Oxford University, 1983.
21 B. O. Loopstra, J. C. Taylor, and A. B. Waugh, *J. Solid State Chem.*, 1977, **20**, 9.
22 S. Siegel and H. R. Hoekstra, *Inorg. Nucl. Chem. Lett.*, 1971, **7**, 455.
23 E. Wait, *J. Inorg. Nucl. Chem.*, 1955, **1**, 309.
24 J. J. Pireaux, J. Riga, E. Thibaut, C. Tenret-Noël, R. Caudano, and J. J. Verbist, *Chem. Phys.*, 1977, **22**, 113.
25 S. P. McGlynn and J. K. Smith, *J. Mol. Spectrosc.*, 1961, **6**, 164.
26 J. J. Verbist. J. Riga, C. Tenret-Noël, J. J. Pireaux, G. d'Ursel, and R. Caudano, 'Plutonium and other Actinides,' North-Holland Publishing Co., Amsterdam, 1976.
27 Yu.A. Teterin, V. M. Kulakov, A. S. Baev, N. B. Nevzorov, I. V. Melnikov, V. A. Streltsov, L. G. Mashirov, D. N. Suglobov, and A. G. Zelenkov, *Phys. Chem. Minerals*, 1981, **7**, 151.
28 G. C. Allen, A. J. Griffiths, and B. J. Lee, *Transition Met. Chem. (Weinheim, Ger.)*, 1978, **3**, 229.
29 G. C. Allen and P. A. Tempest, *J. Chem. Soc., Dalton Trans.*, 1983, 2673.
30 B. G. Hyde, *Acta Crystallogr., Sect. A*, 1971, **27**, 617.

Received 20*th November* 1986; *Paper* 6/2239